STRUCTURAL DESIGN AND OPTIMIZATION OF VACUUM INFUSION MANUFACTURING PROCESS FOR THE FIBERGLASS HOPPER CAR BODY

I.V. Sergeichev [a*], B.N. Fedulov[a], A.A. Safonov[a], A.E. Ushakov[a], N.V. Rozin[b], E.I.Kornienko[b], A.V. Izotov[b], Yu. G. Klenin[b]

[a]*The Skolkovo Institute of Science and Technology, 100, Novaya str., Skolkovo, Moscow, 143025, Russia*
[b]*Scientific and production enterprise ApATeCh ltd, 14/2, Novaya Basmannaya str., Moscow, 107078, Russia*
i.sergeichev@skolkovotech.ru

Keywords: a railway hopper car body, fiberglass composites, finite element analysis.

Abstract
Complete cycle of design and manufacturing of a new railway hopper car 19-5167 with fiberglass body and roof is presented. Structural design, original layups development, FE stress analysis, testing of coupons and subcomponent specimens, an optimization of the vacuum infusion manufacturing process were realized by "ApATech" company in collaboration with Skolkovo Institute Science and Technology for production of the fiberglass hopper car body. FE analysis of the car body structures has been performed for the normative load cases where the applied loads were ordered by the Russian railway regularities. Besides of these cases the impact full scale testing of the body as a part of the car has been simulated via real dynamic contact interaction of the car body structure with a bulk cargo where the structure was modeled by Lagrangian mesh and the bulk cargo was modeled by Eulerian one. The subcomponent specimens were tested under operating conditions to support the structural design and experimental verification of the FE models. To optimize the car manufacturing a numerical modeling of the vacuum infusion process has been realized as well.

1. Introduction

One of the most perspective ways of an evolution of a railway car manufacturing is an application of advanced composite materials on a basement of fiberglass lamina. The major advantages that result from the use of composite materials in the design and fabrication of hopper cars are weight savings, fuel savings and corrosion resistance. Design of the new perspective structures from composite materials requires the both experimental study and FE simulation of regular structural elements and their joints to each other as well. In spite of widespread implementation of fiberglass composites in railroad industry in Europe and USA up to production of a whole car body [1], here is the first experience of, design and manufacturing of the composite hopper car body in Russia.

The car body was produced like two monolithic parts (a roof and a body itself) including the frames and ribs by one cycle of the infusion. The hopper car 19-5167 with fiberglass body and roof is shown at Fig. 1. It has to be mentioned that the JEC group awarded the manufactured hopper car by the Innovation Awards Europe 2014, see http://www.jeccomposites.com/events/innovation-awards-europe-2014 for details.

Figure 1. The manufactured hopper car 19-5167 with fiberglass body and roof

At present work the complete FE analysis of fiberglass hopper car body for transportation of chemical fertilizers, grains and etc. is performed. Based on this analysis the optimal car design has been achieved to satisfy the weight/strength requirements. A development of original fiberglass layups of the car body components, structural design, manufacturing of testing coupons and subcomponent specimens, a corresponding experimental study, a development of the vacuum infusion manufacturing technology were realized by "ApATech" company. The car body is a monocoque structure stiffened by seven inner crossed frames and continuous central beam supporting the end walls. The principal dimensions and characteristics of the car body are given at Table 1. Principal stages of the car body design are:

1. Numerical modeling of the subcomponent specimens' infusion for an adjustment of the technological conditions.
2. Testing of coupons.
3. Manufacturing and testing of the subcomponent specimens.
4. Experimental verification of the analysis methods by the test data.
5. FE analysis of the car body structure and optimization.

Length, mm	**Width, mm**	**Height, mm**	**Car body weight, kg**	**Volume, m^3**	**Carrying capacity, tons**
13700	3220	3920(from unloading bunker) 4230(from rail head)	5380	125	74

Table 1. Dimensions and characteristics of the car body

2. Numerical modeling and optimization of vacuum infusion process

Manufacturing of composite structures by vacuum infusion method has its own advantages, but it requires a detailed analysis of the resin impregnation process [2]. For production of the car body as indivisible monolithic structure without technological defects the advanced methods of modeling of the impregnation are required. As usual, many expensive experiments are necessary for development of final approach to infusion process. To reduce the number of such experiments the numerical modeling of resin propagation has been realized by PAM-RTM software. The impregnation process was modeled on basement of Darcy's law. Resin and fiber properties for infusion simulation are given at Table 2. These properties were obtained from technological experiments conducted by "ApATech" company in according with a method described in [2]. The material components applied for the structure are EQX 1200 multiaxial glass fabrics (stitched) and AROPOL S 604 INF-90 resin.

Resin density	1184 kg/m^3
Resin viscosity	0.0083 Pa sec
Permeability of fiber	K1=7.6e-11 m^2, K2=7.6e-11 m^2, K3=3.6e-12 m^2
Resin/fiber ratio	50%
Resin fill pressure	1e+5 Pa
Vacuuming	5.5e+2 Pa

Table 2. Material properties for infusion simulation

The simulation was realized for the both principal monolithic parts of the car body – the roof and the car body itself. Because of the simulation, it was found out that the roof structure had non-impregnated zones on the final stage of resin infusion (Fig.2, left). Therefore, to prevent the occurrence of the technological defects an additional vacuum channel was setup as shown at Fig. 2 (right).

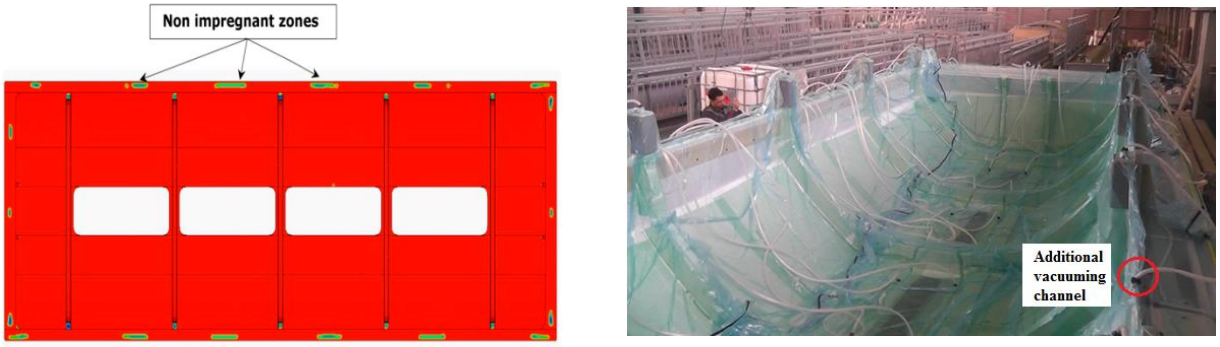

Figure 2. Additional vacuum channels setup

To optimize the resin infusion of the car body itself the step-by-step scheme was developed. The scheme has three levels of resin transportation located at one meter from each other like for linear transportation scheme but this combined scheme has additional channels by length 0.5 meter, which are typical for tree-type scheme (Fig.3).

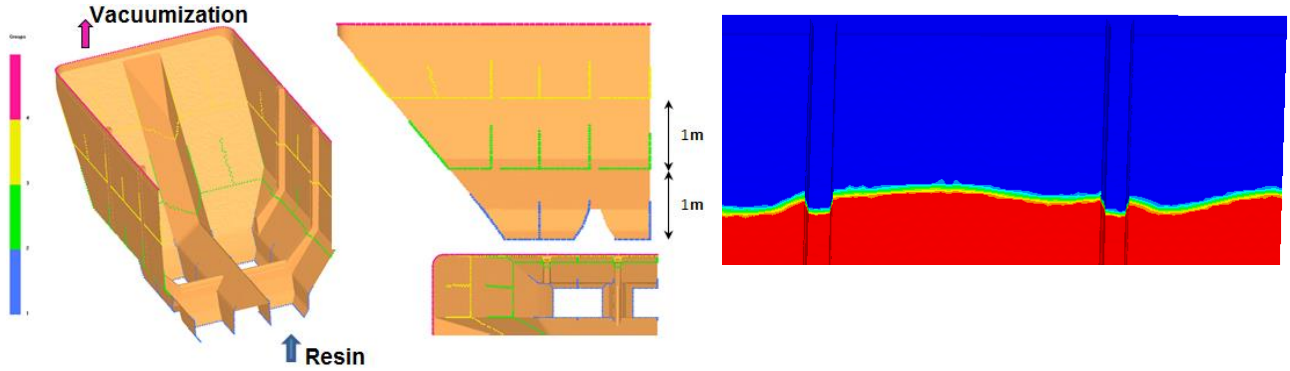

Figure 3. The combined scheme of resin transportation (left) and the location of impregnation front before starting of the third resin transportation level (right)

Lengths of the tree-type appendixes are varied. For example, a length of the channel located at the frame is larger than the channel located between frames (Fig. 3, left). This is due to the frame channel has to impregnate the both skin and frame. After simulation of the impregnation under equal lengths of the appendixes the infusion front delayed a little at the frames in comparison with the front from channels located between the frames as shown at Fig. 3, right. The suggested infusion scheme allows providing a uniform impregnation in 1 hour and 24 minutes as show at Fig. 4 (left).

However, there is some possibility for appearance of non-impregnated zones in the frames (Fig.4) at 667 sec. of the impregnation time. However, these critical zones will have been impregnated at 1800 sec. To avoid such potential defects the additional channels for resin input were setup at the first infusion level as shown at Fig.4 (right). After supplement of these channels, the air traps disappeared from the simulation.

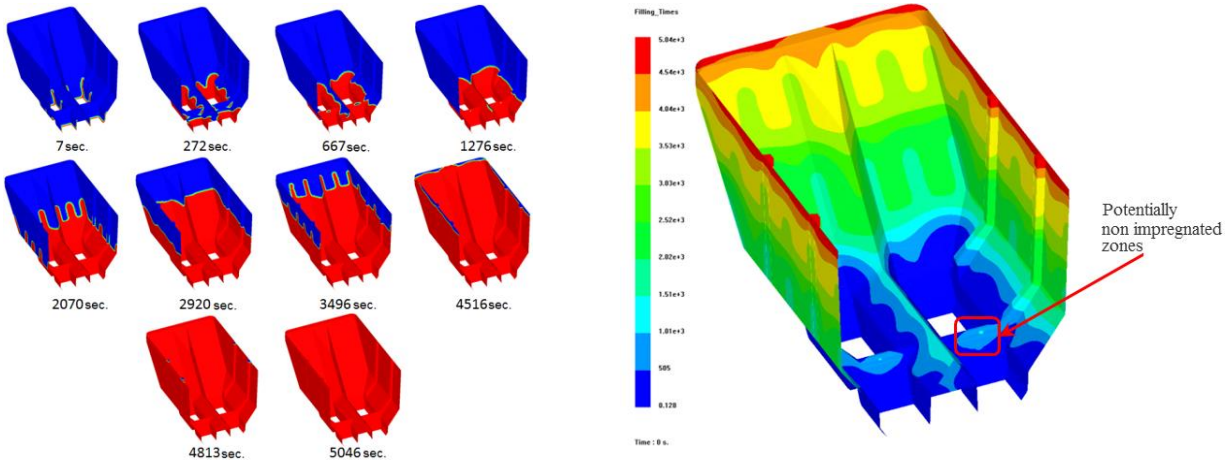

Figure 4. An expansion of the impregnation front (left) in time and the impregnation of the car body (right).

3. Material and subcomponent tests

The car body was infused after preforming of dry glass fibers with implemented Lantor Soric fillers to get a quasi-isotropic composite sandwich. The fillers were applied to increase a bending stiffness of the car body skin and for improving of the impregnation as well. The stiffeners like frames were infused like fiberglass structural elements. Material strength properties and interlaminar fracture toughness obtained by testing of the fiberglass quasi-isotropic coupons are given in Table 3. The material tests were carried out in accordance with corresponding ASTM standards. One of the critical design stages is an experimental and FEM analysis of the non-bolted frame-to-skin joints. This area of the structure is subjected to critical shear load that can cause a delamination and ply failure as well. This shear load arises due to 3.5g normative horizontal overload from cargo inertia pressurized to end wall of the car body itself and its roof. The subcomponent test configuration and experimental facilities are shown at Fig.5. The frame-to-skin specimens were fixed on a rigid metal part which simulates the car underframe. Delamination and ply damage initiation loads were determined in the tests. Several steps applied the shear load. At each step, the delamination area was recorded by means of nondestructive ultrasonic method (C-Scan). The experimentally obtained delamination area plots were used for verification of the applied FE models.

Tension strength, MPa	335
Tension modulus, MPa	19035
Compression strength, MPa	268
Compression modulus, MPa	21241
Shear strength, MPa	36
Shear modulus, MPa	13494
Fracture toughness G_{IC}, N/m	56
Fracture toughness G_{IIC}, N/m	320

Table 3. Fiberglass properties

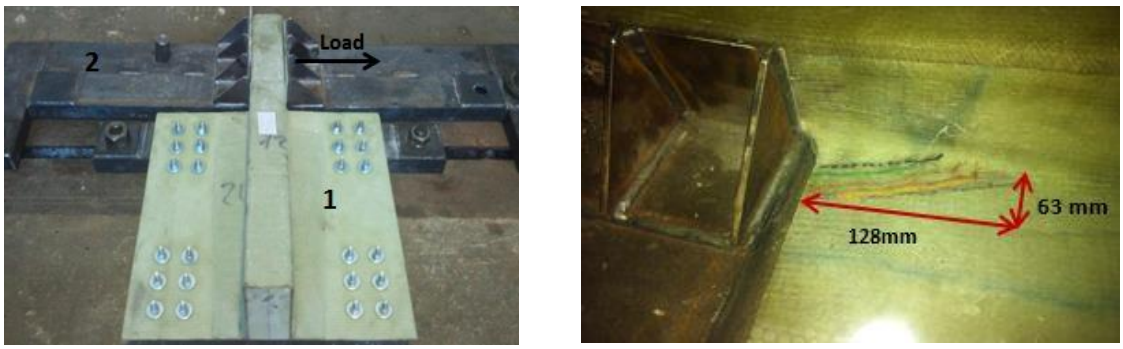

Figure 5. Subcomponent shear test configuration for testing of skin-to-frame joints (left) and delamination area recorded in the test (right)

4. Finite element analysis of the subcomponent tests and verification

To analyze numerically stress-strain state of the subcomponent specimens the corresponding 3D FE models were developed. The modeling of ply damage was realized by Hashin's failure criteria [4] and delamination was modeled by virtual crack closure technique (VCCT) [5]. The stress distribution under the ply damage initiation load is shown at Fig. 6 (left). The calculated load - displacement plot is shown at Fig. 6 (right), where delamination and ply damage initiation loads are marked. Fig.7 shows the experimental and numerical plots of an evolution of delamination area due to the applied loads.

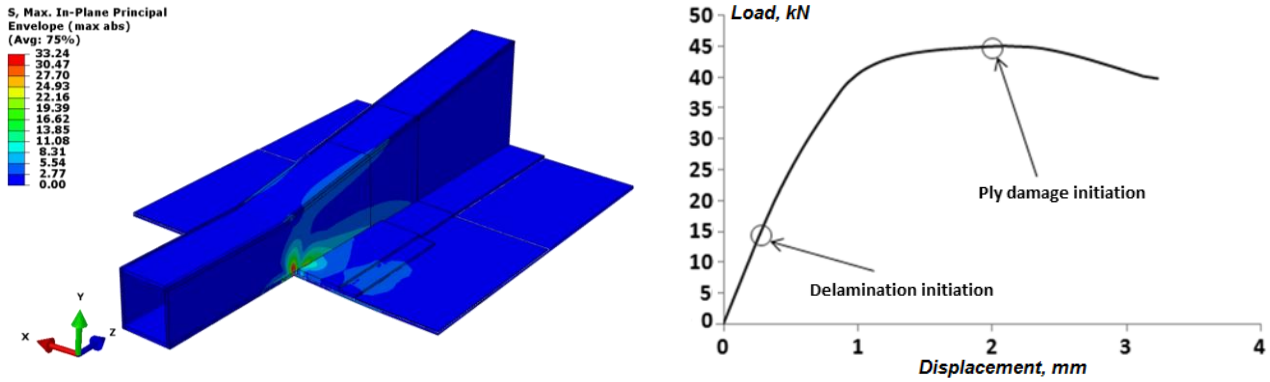

Figure 6. Stress concentration at the skin-to-frame joint, ×9.80665 MPa (left) and the load-displacement plot of skin-to-frame joint testing (right)

From comparison of the testing and simulation data, the applied FE technique provides a good agreement with experiments. The test data has been obtained from non-destructive inspection of the specimen during the test. The recorded growth of the delamination area is given at Fig. 5 (right) where the delamination area at the end of testing are show by the external grey line.

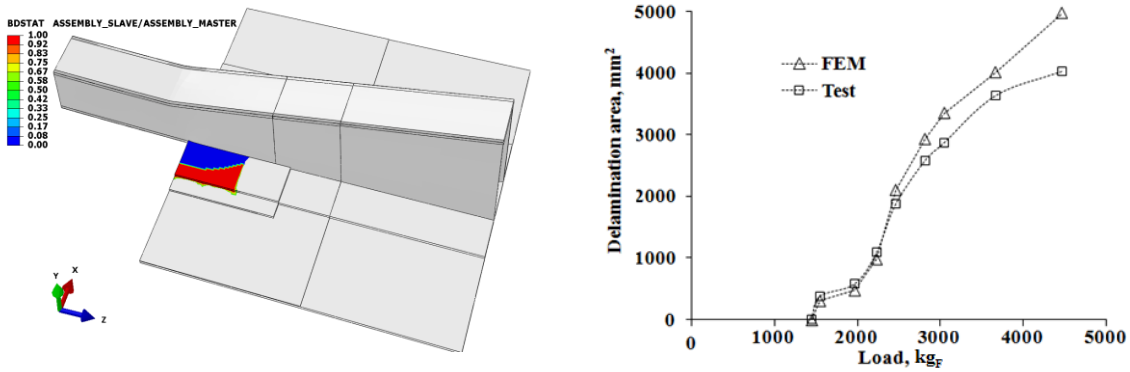

Figure 7. FE simulation of the crack propagation (left) and test vs. FEA delamination area plots (right).

5. FE analysis of the car body structure

Strength analysis of the car body structure was performed for the fully loaded body by 74 tons of 600 kg/m^3 bulk cargo density. The initial conditions of the FE model simulate an impact of the car by 100 tons standard striker-car with velocity 13 kmh. Such dynamic loading corresponds to 3.5g normative horizontal overload from cargo inertia pressurized to front walls of the body itself and the roof. The striker-car was modeled as a rigid undeformable contact surface with an appropriate attached mass. This surface was fixed by a grounded spring with damping behavior corresponding to typical hopper car coupling. The FE simulation was realized by ABAQUS software.

5.1. Modeling of the body structure and bulk cargo interaction

To simulate a deformation of the bulk cargo and its interaction with the car body the Drucker-Prager model was applied [6]. The model parameters are given in Table 4. For stress analysis of the car body a linear elastic model was applied. To take into account a friction between the cargo and the car body structure the friction coefficient was setup to be equal 0.3 at contact options.

Bulk cargo density, kg/m^3	600
Friction angle, radians	0.738
Cohesion, MPa	0.00716
Elasticity modulus, MPa	1.02
Poisson coefficient	0.27

Table 4. Parameters of the applied Drucker-Prager model.

Dynamic interaction of the car body structure with bulk cargo was modeled by Lagrangian-Eulerian approach. The car body is discretized by Lagrangian mesh and the cargo is meshed by Eulerian elements. Such discretization model provides calculation of finite deformation and compaction of the cargo under a movement of its layers during dynamic interaction with the car body structure. The developed FE model is shown at Fig.8. Due to longitudinal symmetry of the problem only one half of the structure was modeled.

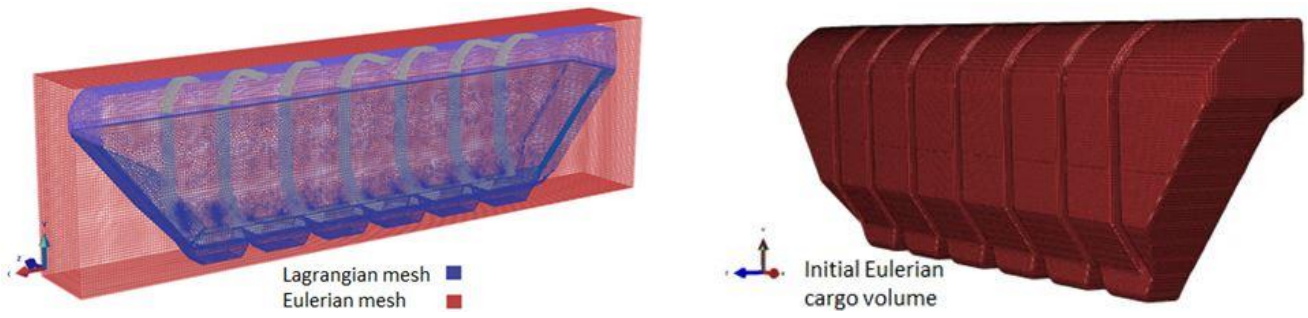

Figure 8. Modeling of interaction of the bulk cargo and the car body structure.

5.2. FE simulation results

Results of the FE simulation are given below as principal stress distributions (max absolute values during a time of deformation) and stress – time plots extracted from elements where the max absolute values achieved. The presented max principal values correspond to maximum tension stress (positive), the min principal stress corresponds to minimum of compression stress (negative). For comparison, the plots are given by their absolute values.

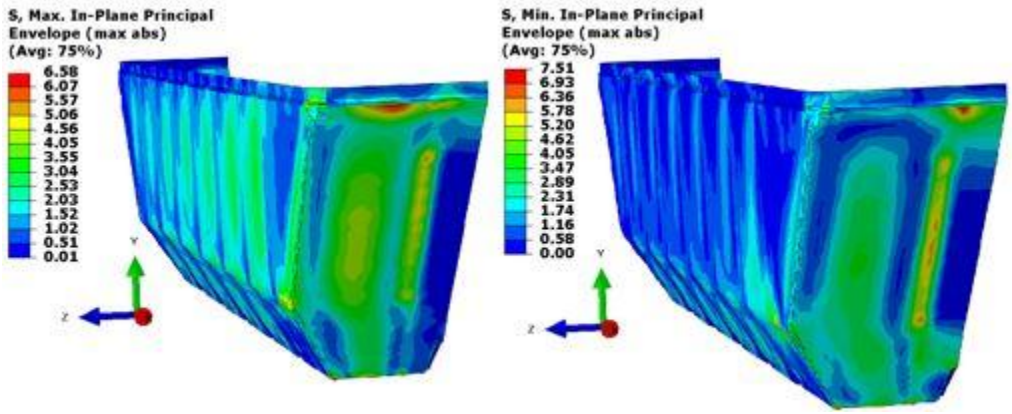

Figure 9. Maximum (*left*) and minimum (*right*) principal stress in the skin of the car body itself (max absolute values during a time of deformation), ×9.80665 MPa

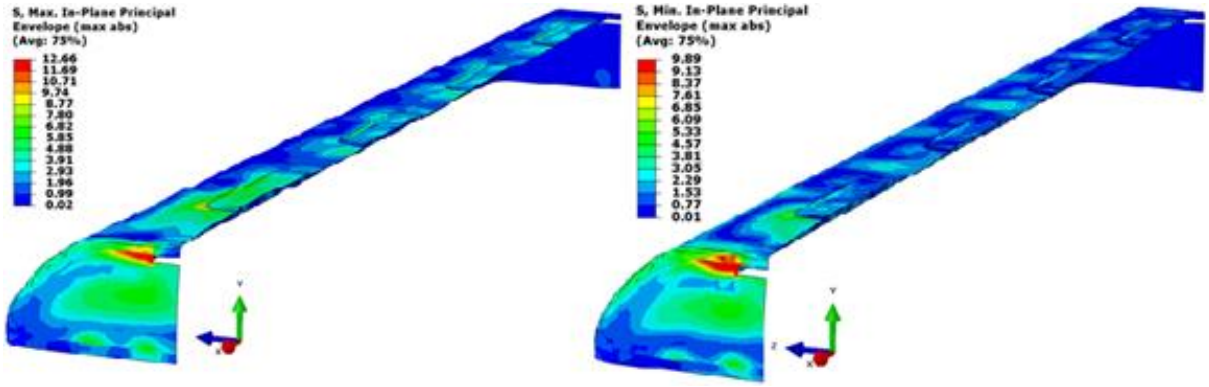

Figure 10. Maximum (*a*) and minimum (*b*) principal stress in the skin of the car roof (max absolute values during a time of deformation), ×9.80665 MPa

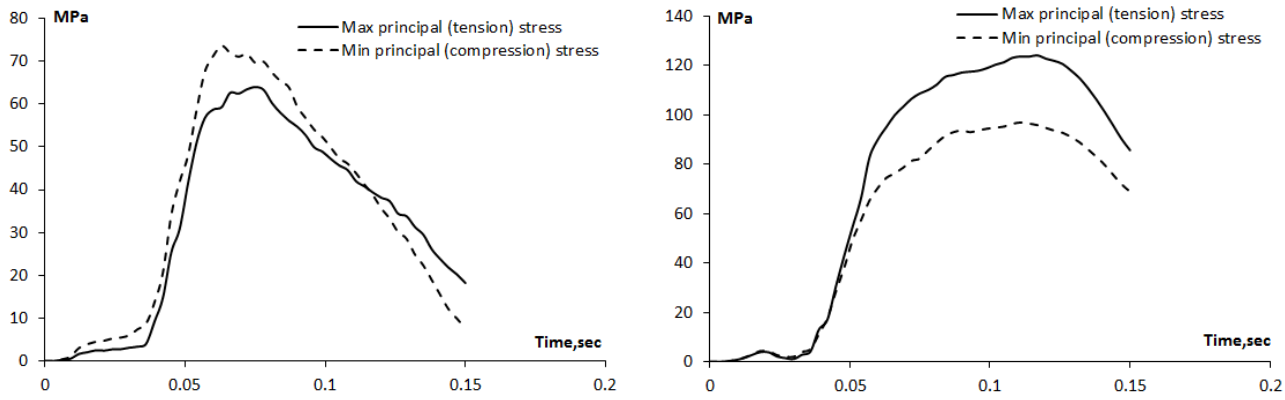

Figure 11. Stress-time plots for the skin of the car body (left) and the roof (right)

It can be mentioned from Table 5 there is a significant difference between stresses in frames obtained from static normative loading analysis and direct impact analysis (blue numbers in the table). Possibly this is due to the normative loading analysis does not take into account of volume increase of the bulk cargo around the frames out of its shear behavior predicted by the applied Drucker-Prager model.

Structural car body element	**Tension**			**Compression**		
	Allowable stress, MPa	**Actual stress, MPa**		**Allowable stress, MPa**	**Actual stress, MPa**	
		Normative load cases	Direct impact simulation		Normative load cases	Direct impact simulation
Roof skin	133	111.9	124.2	106	97.3	97.0
Roof frames		32.0	123.4		35.7	92.6
Car body basement		99.7	89.4		65.9	71.7
Front and side wall of car body skin		79.7	64.5		63.2	73.6
Regular frames of the car body skin		27.9	93.8		32.7	74.2
End frames of the car body skin		31.6	101.6		31.5	89.0
Car body central beam		55.8	88.5		42.6	79.8

Table 5. A comparison of FE results for the normative load application case and the direct impact simulation

6. Conclusions

Complete cycle of design and manufacturing of a new hopper car 19-5167 with fiberglass body and roof was performed. A hybrid linear and tree-type scheme of the resin input was suggested on a basement of numerical simulation and then applied for manufacturing of the real car body structure to optimize the car manufacturing. The subcomponent specimens were tested for verification of the applied modeling approach. FE analysis of the car body structure was performed for the both static normative load case and impact test loading of the car by a standard striker-car.

7. References

[1] D. C. Ruhmann. The design, fabrication and testing of the glasshopper prototype covered hopper rail cars, Composite Structures 27 (1994) 207-213

[2] C.H. Park, A. Lebel, A. Saouab, J. Bréard, W.I. Lee, "Modeling and simulation of voids and saturation in liquid composite molding processes," Composites Part A : Applied Science and Manufacturing, Vol. 42 (6), pp. 658-668, 2011, Elsevier.

[3] Ushakov A.E., Klenin Y.G., Sorina T.G., Kornienko E.I., Safonov A.A. Permeability evaluation of dry fiber preforms designed for vacuum infusion production of composite panels // Composites and Nanostructures. 2013. №1, p. 46-56 (in Russian).

[4] Hashin, Z., "Failure Criteria for Unidirectional Fiber Composites," Journal of Applied Mechanics, vol. 47, pp. 329–334, 1980

[5] Wu E. M., Reuter Jr. R. C., Crack Extension in Fiberglass Reinforced Plastics. T and M Report, University of Illinois, vol. 275, 1965

[6] Drucker, D. C. and Prager, W. (1952). Soil mechanics and plastic analysis for limit design. Quarterly of Applied Mathematics, vol. 10, no. 2, pp. 157–165.